

BLAZING TRAILS: MICROQUASARS AS HEAD-TAIL SOURCES AND THE SEEDING OF MAGNETIZED PLASMA INTO THE ISM

HEINZ, S.

University of Wisconsin-Madison and
Department of Astronomy, 6508 Sterling Hall, 475 N. Charter St., Madison, WI 53593

GRIMM, H.J.

Harvard Smithsonian Center for Astrophysics and
60 Garden St., Cambridge, MA 02138

SUNYAEV, R.A.

Max-Planck-Institute for Astrophysics and
Karl-Schwarzschild-Str. 1, 85741 Garching, Germany

FENDER, R.P.

University of Southampton and
Department of Astronomy, Building B46, Southampton, Hampshire SO17 1BJ, United Kingdom
Draft version August 27, 2021

ABSTRACT

We discuss the dynamics of microquasar jets in the interstellar medium, with specific focus on the effects of the X-ray binaries' space velocity with respect to the local Galactic standard of rest. We argue that, during late stages in the evolution of large scale radio nebulae around microquasars, the ram pressure of the interstellar medium due to the microquasar's space velocity becomes important and that microquasars with high velocities form the Galactic equivalent of extragalactic head-tail sources, i.e., that they leave behind trails of stripped radio plasma. Because of their higher space velocities, low-mass X-ray binaries are more likely to leave trails than high-mass X-ray binaries. We show that the volume of radio plasma released by microquasars over the history of the Galaxy is comparable to the disk volume and argue that a fraction of a few percent of the radio plasma left behind by the X-ray binary is likely mixed with the neutral phases of the ISM before the plasma is removed from the disk by buoyancy. Because the formation of microquasars is an unavoidable by-product of star formation, and because they can travel far from their birth places, their activity likely has important consequences for the evolution of magnetic fields in forming galaxies. We show that radio emission from the plasma inside the trail should be detectable at low frequencies. We suggest that LMXBs with high detected proper motions like XTE J1118+480 will be the best candidates for such a search.

Subject headings: black hole physics — ISM: jets and outflows — X-rays: binaries

1. INTRODUCTION

The interaction of AGN jets with their environments has been under investigation for several decades, partly because it is easily observable through the morphology of radio lobes (e.g. Miley 1980) and X-ray cavities (e.g. McNamara & Nulsen 2007). Because the most powerful AGNs are essentially stationary in the centers of galaxy clusters, models of this interaction typically only consider stationary atmospheres that jets run into (see, e.g., Heinz et al. 2006b for recent work on jets in dynamic atmospheres). The evolution in this case can be separated into three distinct phases: (1) the early momentum driven phase, where the ram pressure of the jet is significant for the dynamical evolution and the source evolves into an elongated structure with narrow cocoons, (2) the energy driven phase, where the slowed-down jet plasma inflates supersonically expanding lobes, excavating a quasi-spherical cavity (this phase is well described by the self-similar solution by Castor et al. 1975; Kaiser & Alexander 1997; Heinz et al. 1998), and (3) the late, sub-sonic evolution, when the radio lobes (the reservoirs of relativistic gas released

by jets) are in pressure equilibrium with the environment. In the case of AGNs, this radio plasma is buoyant in the host galaxy/galaxy cluster atmosphere (see Reynolds et al. 2002, for a more detailed review).

It is becoming increasingly clear that X-ray binaries (XRBs) are also producing relativistic jets over a wide range in accretion rate (Fender & Hendry 2000; Fender & Kuulkers 2001; Gallo et al. 2003; Fender et al. 2004). The inner regions of these XRB jets, where their dynamics is governed by the atmosphere of the compact object powering them, are very similar to the inner regions of AGN jets (Heinz & Sunyaev 2003). However, Heinz et al. (2002) showed that some critical differences exist between XRB jets and AGN jets in how they interact with the larger scale environment, well outside of the sphere of influence of the central compact object. One of the differences is that, in comparison with AGN jets, the ISM poses a much weaker barrier to microquasar jets. This is because the XRB jet thrust (in other words, the ram pressure delivered by the jet) is much larger in comparison to the inertial density of the ISM than it is in the case of AGN jets.

The second fundamental difference between the two cases is, of course, that XRBs do not reside in the centers of dark

matter halos with stratified gaseous atmospheres. Instead, they travel through regular Galactic ISM with some space velocity v_{XRB} , set by supernova kicks and orbital dynamics. The velocity dispersion of XRBs implies that a significant fraction of these sources are moving with large (supersonic) velocities through the ISM, which will have important consequences for their dynamics. VLBI parallax measurements have shown that a microquasars can be moving with velocities in excess of 100 km s^{-1} with respect to the local standard of rest (Mirabel et al. 2001). As a result, the ram pressure of the ISM will act on the radio plasma released by the source, sweeping back the outer layers of the radio lobe.

In this paper, we argue that this aspect has important consequences for the interaction of some XRB jets with their environment: Instead of inflating stationary cocoons, in many cases they will produce trails of radio emitting plasma (made up of relativistic particles and magnetic fields) as they travel through the Galaxy. A very similar situation is encountered in pulsar bow shock nebulae (Cordes 1996; Frail et al. 1996), where a relativistic wind inflates a channel in the ISM through which the pulsar is moving, and, of course, in extragalactic head-tail sources, which are the direct equivalent of jets propagating into a moving medium.

The paper is organized as follows: In §2, we will present a simple parametric model of the interaction of the jets with the ISM. In §3 we discuss the consequences for particle and magnetic field input into the ISM, §4 discussed the observational signatures of this interaction, and §5 presents a brief summary of the paper.

2. THE INTERACTION OF MICROQUASAR JETS WITH THEIR ENVIRONMENT

No detailed, global models of the dynamical interaction of XRB jets with the ISM exist as of yet. In the absence of such models, the first logical step is to explore a relatively simple sketch of how this interaction occurs. The predictions we will make are based on what we know about the interaction of AGN jets with their environment, some insight gained from the scaling relations derived in Heinz et al. (2002) and on the estimates of the kinetic energy output from these source derived in Fender et al. (2005) and Heinz & Grimm (2005, HG05 hereafter).

Throughout the paper, we will assume that the dynamical time of the large scale evolution of the source is long compared to the variability time scale of the XRB and the jet (see §2.1). This will allow us to neglect the variable nature of the jet power in the long term evolution of the large scale radio lobe and instead use a time averaged constant value.

Based on the estimated power $W_{\text{cyg}} \sim 10^{37} \text{ ergs s}^{-1}$ of the jet in Cyg X-1 from Gallo et al. (2005), and loosely guided by the limit on the average jet power of $\langle W \rangle \sim \text{few} \times 10^{37} \text{ ergs s}^{-1}$ from HG05¹, we adopt a fiducial ensemble average kinetic jet power *per source* of

$$\mathcal{W} \equiv \langle W \rangle \equiv 10^{37} \text{ ergs s}^{-1} \cdot W_{37} \quad (1)$$

We will also use the estimated average aggregate power from *all* XRB jets of $W_{\text{tot}} \sim 5 \times 10^{38} \text{ ergs s}^{-1}$. This estimate does *not* include the even more uncertain contributions from neutron star jets or optically thin radio outbursts, both of

¹ The average power in HG05 was derived from a limited luminosity range, excluding sources below the luminosity completeness limit, inclusion of which would bring the average down.

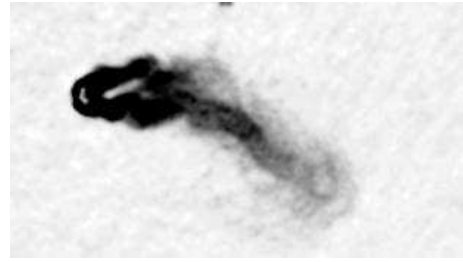


FIG. 1.— Radio map of extragalactic head-tail source 3C83.1 (NGC 1265), rotated by 90 degrees (Odea & Owen 1986).

which will increase the total power and thus the importance of the effects discussed here.

We will further assume that the gas is sufficiently ionized or sufficiently dense to treat the magnetized plasma released by the jet and its environment as fluids and use hydrodynamic arguments (see §3.2).

We will use a set of fiducial parameters for the ISM. Since the ISM itself is turbulent and inhomogeneous we cannot simply assign a mean density. We will discuss the three putative main phases (cold, warm, and hot) separately whenever appropriate. The ISM pressure is likely dominated by turbulent pressure and contains contributions from thermal and non-thermal particles and magnetic fields. We will use a fiducial mean total ISM pressure of (Cox 2005)

$$p_{\text{ISM}} \approx 3 \times 10^{-12} \text{ ergs cm}^{-3} \cdot p_{-11.5} \quad (2)$$

We will assume throughout the paper that the working surface, i.e., the place where jet and ISM interact directly, slowing down the jet material (taken to be a strong terminal shock²) is efficient at slowing the jets down to sub-relativistic velocities and thus dissipating most of the kinetic energy into internal energy of the radio plasma. For a jet with length l_{jet} and half opening angle $\alpha \equiv 1^\circ \alpha_1$ (where α_1 is the opening angle measured in degrees), this is the case for

$$l_{\text{jet}} \gtrsim 10^{16} \text{ cm} \cdot \sqrt{\frac{W_{37}}{n_1} \frac{1}{\alpha_1}} \quad (3)$$

where we define the ISM particle density as $n_1 \equiv n_{\text{ISM}}/1 \text{ cm}^{-3}$. The size scales we are interested in are much larger than this, so we are justified in assuming the working surface dissipates most of the kinetic energy. We will also assume that this plasma does not mix with the ISM due to magnetic flux freezing (see, however, §3.2).

2.1. Early evolution

During the early lobe evolution the ISM pressure p_{ISM} , buoyancy forces, and the ISM ram pressure $\rho_{\text{ISM}} v_{\text{XRB}}^2$ due to the space velocity v_{XRB} of the XRB are negligible compared to the ram pressure $\rho_{\text{ISM}} v_{\text{R}}^2$ on the lobe due to its radial expansion velocity v_{R} . It is then appropriate to use the well-known 1-dimensional energy-driven bubble model (Castor et al. 1975; Kaiser & Alexander 1997; Heinz et al. 1998; Gallo et al. 2005) as sketched in Fig. 2. This model assumes that the XRB releases relativistic plasma in a spherically symmetric fashion³

² There is little fundamental difference if instead the jet material is decelerated through a series of weak shocks along the jet

³ This assumption is motivated by the fact that the internal sound speed in a relativistic plasma is much larger than the expansion velocity of the ra-

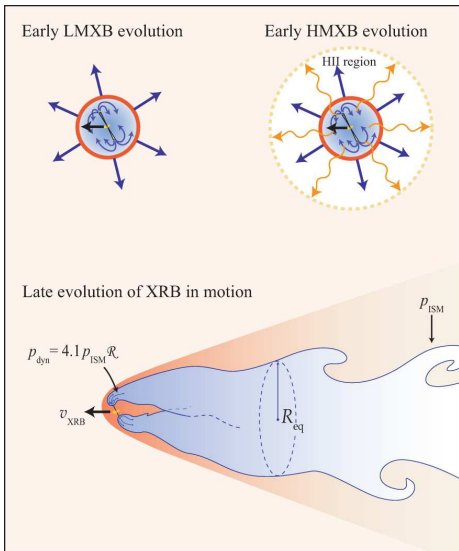


FIG. 2.— Sketch of early and late evolutionary phases in XRB radio lobe dynamics. Note that in the early stages the expansion velocity of the plasma is much faster than the space velocity of the XRB, thus the evolution is quasi-spherical. Later, the ram pressure due to the XRB space velocity and the thermal pressure of the ISM dominate, and the stripped plasma leaves a trail behind the XRB.

Assuming (a) an adiabatic equation of state, (b) uniform pressure for the radio plasma inside the lobe, (c) ram pressure balance with the ISM, and (d) energy conservation, the Castor solution is

$$R_{\text{early}} \approx 0.65 \left(\frac{\langle W \rangle t^3}{\rho_{\text{ISM}}} \right)^{1/5} \quad (4)$$

Apart from the expected synchrotron emission from inside the radio lobe, the supersonic expansion into the ISM will also lead to thermal emission from the shocked ISM shell (Kaiser et al. 2004), similar to expanding supernova remnants. Shocks are extremely valuable as diagnostic tools, since the shock strength measures the expansion velocity of the source, which, when coupled with the source size, can tell us the age and average kinetic power of the source. An example of such a source is Cyg X-1, for which this thermal emission has been detected (Gallo et al. 2005).

2.2. Late evolution: Head-tail sources

At sufficiently late times (the case we are interested in here) the jets will have traveled sufficiently far for the dynamical pressure due to the XRB motion to become important.

The dynamical pressure of the XRB motion through the ISM with velocity v_{XRB} will become comparable to the jet thrust (i.e., the momentum flux along the jet) when the advance speed of the working surface equals the space velocity of the source, $v_{\text{head}} = v_{\text{XRB}}$. If this condition is satisfied, the working surface can no longer advance in the direction of the jet and will thus become stationary in the frame of the XRB.

dio lobe. Thus, regions of overpressure (i.e., the working surfaces of the jets, where the jets interact with the ISM) will quickly distribute their overpressure within the relativistic plasma cocoon (e.g. Begelman & Cioffi 1989). Furthermore dynamical instabilities and precession are believed to spread the jet thrust out over a much larger solid angle than subtended by the opening angle of the jet for the case of AGN jets (Scheuer 1982), driving the aspect ratio of lobes toward unity. We will assume that the effective half opening angle is $\theta = \sqrt{\Omega/\pi} \sim 20^\circ$ (e.g. Young et al. 2005) where Ω is the solid angle swept out by precession and jitter of the jet axis.

Given our fiducial sound speed of $c_{\text{sound}} = 17 \text{ km s}^{-1}$ we will express the XRB's space velocity as

$$v_{17} \equiv \frac{v_{\text{XRB}}}{17 \text{ km s}^{-1}} \quad (5)$$

The shock jump conditions and pressure balance across the working surface (the terminal shock) imply that this happens when the jet thrust

$$p_{\text{jet}} = \frac{5\Gamma + 3}{\Gamma v_{\text{jet}}} \frac{W_{\text{jet}}}{12\pi(\theta l)^2} \quad (6)$$

equals the total dynamic pressure

$$p_{\text{dyn}} = 4.1 p_{\text{ISM}} \mathcal{R}_M \quad (7)$$

$$\mathcal{R}_M \equiv \left\{ 9 + 10M^2 \left[1 + \sqrt{1 + 9/(4M^2)} \right] \right\} / 37$$

of the ISM, where $M \equiv v_{\text{XRB}}/c_{\text{sound}}$ is the effective Mach number of the XRB's motion through the ISM with respect to the effective sound speed of the ISM, $c_{\text{sound}} = \sqrt{5p_{\text{ISM}}/3\rho_{\text{ISM}}}$. We adopt a fiducial value of $\Gamma \equiv 5\Gamma_5$ for the bulk Lorentz factor of the jet, which is, however, of little importance throughout the rest of the paper.

The expression for p_{dyn} in eq. (7) can easily be derived from the shock jump conditions on each side of the working surface (e.g. Blandford & McKee 1976), with non-relativistic equations of state for the unshocked cold jet and ISM gas⁴.

The two dynamical pressures p_{dyn} and p_{jet} are equal when the length of the jets reaches

$$l_{\text{jet}} = \frac{6 \times 10^{18} \text{ cm}}{\theta_{20}} \cdot \left[\frac{W_{37} 25\Gamma + 15}{p_{-11.5} 28\Gamma\beta\mathcal{R}_M} \right]^{1/2} \quad (8)$$

where the expression in brackets is unity for $M = 1$ and the fiducial parameters and $\beta = v_{\text{jet}}/c$. At this length, the working surface becomes stationary in the frame of the XRB, and since the ISM is moving at velocity v_{XRB} with respect to the XRB, the plasma that is released at the working surface must be swept back away from the XRB with the ISM at velocity v_{XRB} and create a trail of “debris” plasma, left behind by the XRB jets.

The time for the jet to propagate that far into the ISM is approximately $t_{\text{eq}} \approx l_{\text{jet}}/v_{\text{XRB}} \approx 10^5$ yrs, which is long compared to typical accretion disk time scales (e.g. Frank et al. 2002) but still short compared to typical companion (i.e., XRB) lifetimes. It is therefore necessary to further discuss this quasi stationary phase of the large scale dynamics of radio plasma released by XRBs (it is quasi stationary since the XRB space velocity v_{XRB} and the local ISM density n_{ISM} change as the XRB traverses the Galaxy).

2.3. The debris: Radio trails

As mentioned above, we assume that the working surface is stationary in the frame of the XRB. Its propagation velocity into the ISM must therefore be v_{XRB} and its pressure must be given by p_{dyn} from above.

The energy released by the jet at the working surface must then equal the jet power:

$$W_{\text{jet}} = \frac{\gamma}{\gamma - 1} p_{\text{dyn}} \frac{dV_{\text{head}}}{dt} \quad (9)$$

⁴ The $\gamma = 5/3$ equation of state is not a crucial assumption and can easily be modified to reflect a relativistic equation of state of the jet gas (for example). The coefficients only change slightly and the qualitative results are unaltered.

where V_{head} is the volume of plasma streaming out of the working surface. The factor $[\gamma_{\text{ad}}/(\gamma_{\text{ad}} - 1)]p_{\text{dyn}}$ is the post-shock enthalpy of the jet plasma and includes both the internal energy $p dV/(\gamma_{\text{ad}} - 1)$ of the plasma released and the $p dV$ work done on the ISM. Since $\gamma_{\text{ad}} = 4/3$ for the jet plasma, the volumetric rate at which jet plasma is released at the working surface is

$$\frac{dV_{\text{head}}}{dt} = \frac{W_{\text{jet}}}{4 p_{\text{dyn}}} \quad (10)$$

Since far downstream (along the swept back trail of radio plasma away from the source) the pressure has to equal the ISM pressure (otherwise the energy in the Mach cone behind the XRB would diverge), the radio plasma originally released at pressure p_{dyn} must expand adiabatically (thus doing further work on the ISM). Thus, the asymptotic volumetric rate at which plasma enters the trail is

$$\frac{dV}{dt} \approx \frac{W_{\text{jet}}}{4 p_{\text{dyn}}} \left(\frac{p_{\text{dyn}}}{p_{\text{ISM}}} \right)^{\frac{1}{\gamma_{\text{ad}}}} = \frac{W_{\text{jet}}}{4 p_{\text{dyn}}} \left(\frac{p_{\text{dyn}}}{p_{\text{ISM}}} \right)^{3/4} \quad (11)$$

In order to estimate the asymptotic lateral radius R_{eq} of the trail (approximated as a cylinder around the XRBs trajectory) from its inflation rate (eq. 11), we need to know the asymptotic flow velocity v_{tr} of radio plasma through the trail. The pressure gradient behind the bow shock (from the ISM ram pressure p_{dyn} to p_{ISM}) will accelerate the plasma along the channel.

In principle, it is possible that the plasma will pick up most of its original outflow velocity and reach mildly relativistic speeds. For example, Bucciantini et al. (2005) investigated the dynamics of pulsar bow shock nebulae using axisymmetric 2.5D relativistic MHD simulations and found that the velocity inside the channel reaches values up to $0.6c$. They concluded, on the basis of their simulations, that the channel width should be comparable to the standoff distance between the pulsar (or XRB in our case) and the stagnation point at the head of the shock. However, the enforced symmetry in their model makes the solution they found over-stable. In reality, it is likely that dynamical instabilities (e.g., Kelvin-Helmholtz or kink instabilities, depending on the strength and topology of the magnetic field) would disrupt such rapid flow through the channel.

We expect the average flow velocity to be roughly that of the ISM sheet around the channel. Asymptotically, this velocity must be v_{XRB} (otherwise the total kinetic energy would diverge). Thus, we will assume that the plasma, far downstream from the XRB will have a flow velocity of $v_{\text{tr}} \equiv v_{\text{XRB}} \mathcal{V}$ with $\mathcal{V} \gtrsim 1$.

Note that even in the case of $\mathcal{V} \gg 1$, the plasma must still come to rest in the ISM at some point, where it would inflate a bubble. This would be around the birthplace of the XRB or around any major change in environmental parameters (i.e., changes in ISM density or pressure), where the channel width would change significantly, leading to a series of ‘‘sausage link’’ bubbles, connected by narrow channels. Note also that the total volume of plasma released should not be affected.

The equilibrium radius R_{eq} of the roughly cylindrical trail is then

$$\begin{aligned} R_{\text{eq}} &\approx \sqrt{\frac{dV}{dt} \frac{1}{\pi v_{\text{XRB}} \mathcal{V}}} \\ &\approx 2 \times 10^{20} \text{ cm} \cdot \sqrt{\frac{W_{37}}{p_{-11.5} v_{17} \mathcal{V}}} \mathcal{R}_M^{-\frac{1}{8}} \end{aligned} \quad (12)$$

This is much larger than the value of l_{jet} (eq. 8). Thus, the ultimate cross section of the trails is much larger than the equilibrium length of the jets and our assumption that both jets are feeding a single trail is justified (this is not qualitatively important for our argument, however).

It is worth pointing out the implicit weak dependence of R_{eq} on density through $\mathcal{R}_M^{-1/8}$ which implies that the size scale of the trails produced should be similar in different environments - an increase in density by three orders of magnitude (with otherwise identical parameters, i.e., pressure and jet power) only reduces R_{eq} by a factor of 3.5, while a decrease in density by three orders of magnitude (i.e., a hot ISM phase environment) only increases R_{eq} by a factor of 1.3. Thus, the most significant effects on R_{eq} are likely to come from $W_{37.3}$, $p_{-11.5}$, and v_{17} .

For a binary lifetime of $t \equiv t_8 \times 10^8$ yrs (where t_8 is the age of the source in units of 10^8 yrs), the length of the trail left by the source is

$$l_{\text{trail}} = 5 \times 10^{21} \text{ cm} \cdot v_{17} t_8 \quad (13)$$

Based on this expression, a source will produce a significant plasma trail if $l \gg R_{\text{eq}}$, or

$$t_8 p_{-11.5}^{1/2} v_{17}^{3/2} \mathcal{V}^{1/2} W_{37}^{-1/2} \mathcal{R}_M^{\frac{1}{8}} \gg 0.06 \quad (14)$$

If this condition is not satisfied, the source dynamics are better approximated as spherical and stationary (if significant gradients exist in the environment of the XRB, the source evolution will, of course, still deviate from a quasi-spherical, symmetric case, as might be the case in Cygnus X-1).

The fiducial values used in eq. (14) are appropriate for LMXBs, implying that LMXBs typically leave trails in the ISM, especially the high velocity tail of the LMXB population with $v_{17} \gg 1$. Since HMXBs have low space velocities and short lifetimes, this condition is typically *not* satisfied for HMXBs: For a characteristic HMXB velocity of $v_{17} \mathcal{V} \sim 0.35$ and a companion lifetime of $t_8 \lesssim 0.1$, the expression on the left is 0.015. Thus, HMXBs typically should *not* produce trails, except for very low power source, and sources in the very high velocity tail of the HMXB distribution in dense, high pressure environments (such as the Galactic center).

In arguments above we have implicitly assumed that a fluid treatment is valid, i.e., that the relativistic particles released by the jet interact collectively with the ISM. This is equivalent to assuming that the particles are frozen to the plasma and that microscopic mixing between ISM and trail plasma is not a dominant effect. We will discuss this assumption and its validity in more detail in 3.2. Any significant amount of mixing will only make the conclusions we will draw below about seeding of magnetic fields into the ISM stronger (however, it might alter the observation appearance of trails as well).

3. MIXING AND THE IMPACT ON THE ISM

Given the estimates for the properties of the radio lobes and trails produced by the ensemble of Galactic XRBs, we can estimate their impact on the ISM. Before going into detail, we will lay out our assumptions about the ISM that the XRBs are interacting with:

For the XRB velocities, we will use a Maxwellian distribution with mean velocities of $\sigma_{\text{H}} \approx 6 \text{ km s}^{-1}$ and $\sigma_{\text{L}} \approx 16 \text{ km s}^{-1}$ for HMXBs and LMXBs respectively, which reproduces the scale heights of both populations. A fraction of about $f_{\text{disk}} \sim 75\% f_{\text{disk},75}$ of the LMXBs reside in the Galactic disk.

For the ISM density distributions we will use volume filling fractions of $f_{\text{hot}} \approx 70\%$, $f_{\text{warm}} \approx 25\%$, and $f_{\text{cold}} \approx 5\%$ for the hot, warm, and cold phases respectively (McKee & Ostriker 1977). We will assume that LMXBs are randomly distributed among the three phases since they are old enough to have moved far enough away from their birth places to have forgotten about their initial environments. HMXBs do not live long enough and have velocities too small to have traveled very far from their birth place, about 60 pc for $v_{\text{XRB}} = 6 \text{ km/s}$ and a life time of 10^7 yrs . This has to be compared to typical molecular cloud size of about 100 pc. We will thus assume that $f_{\text{cold}} = 100\%$ for HMXBs to be conservative (smaller values of f_{cold} will lead to larger values of the total volume of plasma released by HMXBs below).

3.1. The total volume of radio plasma released into the Galaxy

The total volume in radio trails produced by XRBs depends on the distribution of v_{XRB} and ρ_{ISM} only through $\mathcal{R}^{1/4}$. Thus, estimates of the volume of plasma released by jets will be robust against uncertainties in those quantities.

With the ISM parameters given above, the volume in trails produced by the LMXB disk population is simply the current rate of volume injection per LMXB, averaged over the velocity distribution of LMXBs, multiplied by the number of LMXBs, multiplied by the age of the LMXB population $t_{\text{L}} \equiv \times 10^{10} t_{10} \text{ yrs}$.

Using the estimated total integrated kinetic power of the LMXB population of $W_{\text{L}} \approx 3.5 \times 10^{38} W_{\text{L},38.5}$, this gives:

$$\begin{aligned} V_{\text{LMXB,disk}} &\approx W_{\text{L}} t_{\text{L}} \langle (p_{\text{dyn}}/p_{\text{ISM}})^{3/4} / (4p_{\text{dyn}}) \rangle \\ &\approx 5.5 \times 10^{66} \text{ cm}^3 \cdot \frac{W_{\text{L},38.5} f_{\text{disk},75} t_{10}}{p_{-11.5}} \\ &\quad \cdot h_{\text{L}}(\sigma_{\text{L}}, f_{\text{cold,warm,hot}}) \end{aligned} \quad (15)$$

where h_{L} is unity for our fiducial parameters and a very slowly varying function of σ_{L} , n_1 , and $f_{\text{cold,warm,hot}}$ over the parameter range considered. The velocity dispersion σ_{L} drops out of eq. (15) to lowest order. Clearly, the most uncertain parameter left is $W_{\text{LMXB},38.5}$, on which V_{tot} depends linearly.

Taking $f_{\text{hot}} = 100\%$ for the halo population, the volume produced by the halo LMXBs is about $V_{\text{L,halo}} \approx 2 \times 10^{66} \text{ cm}^3 / p_{-11.5}$. However, a sizeable fraction of the plasma produced in the disk will eventually leak into the halo (see below). Since $p_{-11.5}$ is much smaller in the halo than it is in the disk, the total volume filled by plasma released by halo LMXBs and that emanating buoyantly from the disk (see below) is thus likely much larger than this estimate.

For the HMXBs, the total volume rate should be integrated over the star formation rate history, assuming a current star formation rate of $3 M_{\odot} \text{ yr}^{-1} \dot{M}_3$ (where \dot{M}_3 is the Galactic star formation rate in units of 3 solar masses per year).

With the slightly lower value of the total power W_{H} and the total star formation rate integral of $\int dt \dot{M}_{\text{SFR}} = M_{\text{Gal}} \equiv 10^{11} M_{\odot} M_{11}$ (where M_{11} is the Galactic stellar mass in units of 10^{11} solar masses), this gives

$$V_{\text{H,disk}} \approx 4 \times 10^{66} \text{ cm}^3 \cdot \frac{W_{\text{H},38.3} M_{11}}{p_{-11.5} \dot{M}_3} h_{\text{H}}(\sigma_{\text{H}}, f_{\text{c}}) \quad (16)$$

Again h_{H} is slowly varying.

Summarizing, the total volume of radio plasma released into the disk by XRB jets over the lifetime of the Galaxy is then roughly $8 \times 10^{66} \text{ cm}^3$, and the volume released by halo LMXBs is roughly $2 \times 10^{66} \text{ cm}^3 \times (p_{\text{disk}}/p_{\text{halo}})$.

This should be compared to the disk and the halo volumes: Taking the disk scale height to be 500 pc and the disk radius to be 10 kpc, the disk volume is $V_{\text{disk}} \approx 10^{67} \text{ cm}^3$, while the halo volume is roughly $V_{\text{halo}} \gtrsim 10^{68} \text{ cm}^3$. Clearly, XRBs will have released sufficient relativistic plasma to fill a significant fraction of the disk and even the halo. If the radio plasma were confined to the disk, it would fill up to 100% of the disk (and could account for all of the hot ISM phase in the disk). This immediately implies that the buoyancy of this plasma in the vertically stratified Galactic gas will eventually move most of the trails out into the halo. It also implies that a volume fraction larger than 10% of the halo might be filled with radio plasma produced by XRBs. We will discuss further implications of this result below.

3.2. Microscopic mixing

Microscopic mixing of radio plasma and ISM is only going to be important in sufficiently neutral ISM phases, since otherwise the strong magnetization of the trail plasma will effectively decouple both phases.

While the ISM will be sufficiently ionized near the working surface, it might well be neutral far back along the trail. In this case, neutral particles can enter the trail. The cross section for collisional interaction between the neutral particles and the cosmic rays of the trail is negligible. Thus, the only way for neutral ISM particles to interact at all with the trail plasma is through interaction with ionized ISM particles via ambipolar diffusion and charge exchange reactions (we will ignore the latter given the expected low cross sections).

While a detailed discussion of microscopic mixing of relativistic plasma across radio lobe boundaries is beyond the scope of this paper, we will briefly present an order of magnitude estimate of the importance of ambipolar diffusion of neutral ISM into XRB radio lobes and trails to show that the expected amount of mixing is astrophysically interesting.

Following Draine et al. (1983), we use a constant ion drag coefficient of $\gamma_{\text{ion}} = 3.5 \times 10^{13} \text{ cm}^3 \text{ g}^{-1} \text{ s}^{-1}$. In the cold neutral phase, it is appropriate to use an ionization fraction of $\xi_i = n_i/n_n = C_i \rho_n^{-1/2}$ with $C_i \approx 3 \times 10^{-16} \text{ g}^{1/2} \text{ cm}^{-3/2}$ (Elmegreen 1979). In the warm neutral medium, the ionization fraction is higher, of order $\xi_i \approx 10\%$ (e.g. Dalgarno & McCray 1972).

Next, we need to estimate the field strength inside the trail. Given the estimated pressure and size of the plasma trail, we can parameterize the field strength in terms of its equipartition value,

$$\begin{aligned} B_{\text{eq}} &= \sqrt{3\xi_B 8\pi p_{\text{trail}} / (1 + \xi_B)} \\ &\approx 11 \mu\text{G} \cdot \sqrt{2\xi_B p_{-11.5} / (1 + \xi_B)} \end{aligned} \quad (17)$$

where ξ_B is the ratio of magnetic to particle pressure and p_{tot} is the total (particle plus magnetic) pressure. For simplicity, we assume the field is tangled isotropically, leading to the additional factor of 3 (e.g. Heinz & Begelman 2000).

The ambipolar diffusion coefficient for cold neutrals entering the trail/lobe is then (e.g. Shu 1992)

$$D_{\text{amb,cold}} = \frac{v_{\text{A}}^2}{\gamma \rho_i} = \frac{B^2}{4\pi \rho_n \gamma C_i \rho_n}$$

$$\approx 4 \times 10^{20} \text{ cm}^2 \text{ s}^{-1} \cdot p_{-11.5} \left(\frac{10^4 \text{ cm}^{-3}}{n_n} \right)^{3/2} \frac{2\xi_B}{1 + \xi_B}$$

and for warm neutrals

$$D_{\text{amb,warm}} = 10^{24} \text{ cm}^2 \text{ s}^{-1} \cdot \frac{p_{-11.5}}{n_n^2} \frac{10\%}{\xi} \frac{2\xi_B}{1 + \xi_B} \quad (18)$$

We are interested in the asymptotic mixing fraction far back along the trail, when it has reached its equilibrium radius. Thus, we will not consider dynamical effects due to the trails initial expansion on the total mixing fraction⁵.

A conservative assumption about the longevity of the radio trail is that it will last at least one sound crossing time against any dynamical instabilities (see §3.3). Within a sound crossing time $\tau_{\text{sound}} = R_{\text{eq}}/c_{\text{sound}}$, the ambipolar diffusion length is

$$R_{\text{amb}} \approx \sqrt{\frac{D_{\text{amb}}}{\tau_{\text{sound}}}} \quad (19)$$

Thus, a lower limit to the mixing fraction of thermal material from the cold neutral phase into radio trails/lobes produced by microquasars is

$$\begin{aligned} f_{\text{mix,cold}} &\equiv \frac{V_{\text{mix}}}{V_{\text{tot}}} \approx 2 \frac{R_{\text{amb}}}{R_{\text{eq}}} \geq 2 \frac{\sqrt{D_{\text{amb}} \tau_{\text{sonic}}}}{R_{\text{eq}}} \quad (20) \\ &\geq 2\% \cdot \sqrt{\frac{n_1}{10^4}} \sqrt{\frac{1 + \xi_B}{2\xi_B}} \left(\frac{W_{37}}{p_{-11.5}^2 v_{17} \mathcal{V}} \right)^{1/4} \mathcal{R}^{-1/16} \end{aligned}$$

and for warm neutrals

$$\begin{aligned} f_{\text{mix,warm}} &\geq 10\% \sqrt{\frac{\xi_i}{10\%}} \cdot \left(\frac{n_1^3 W_{37}}{p_{-11.5}^2 v_{17} \mathcal{V}} \right)^{1/4} \\ &\cdot \mathcal{R}^{-1/16} \sqrt{\frac{1 + \xi_B}{2\xi_B}} \end{aligned}$$

We conclude that, for the warm and cold neutral ISM, the magnetic field inside the trail presents only a moderate barrier and mixing could be relatively efficient, quickly creating a boundary layer of a few percent thickness around the trail/lobe. At the same time, ambipolar diffusion is probably not strong enough to affect the dynamics of the radio plasma on a global scale.

In conclusion, mixing is significant in the neutral ISM phases, with mixing fractions of order of a few percent. It is likely orders of magnitude smaller for XRBs in ionized environments⁶. This suggest that the global average of f_{mix} should be about a factor of 10 smaller than the volume filling fraction of neutral gas in the Galaxy. So, given recent estimates of volume filling factor of up to 40% for the warm neutral phase (Heiles & Troland 2003) we “guesstimate” a globally averaged mixing fraction of order $f_{\text{mix}} \lesssim 4\%$.

3.3. Competing destruction processes

As the radio plasma expands into the ISM a number of processes will compete to either mix the two phases or remove the plasma from the Galactic disk into the halo.

⁵ During the radial expansion phase of the lobe and in the radially expanding section of the trail, ambipolar diffusion will only work as long as the diffusion speed is faster than the expansion velocity

⁶ Anomalous diffusion can lead to significant mixing even between two completely ionized phases (e.g. Narayan & Medvedev 2001).

3.3.1. Buoyancy

The ISM is vertically stratified due to the gravitational field of the Galaxy. The low density radio trails are buoyantly unstable in this gas, which will drive them upward, away from the Galactic plane.

The buoyancy time scale for a cylindrical trail of radius R is set by the downward ISM dynamical pressure and the upward buoyancy of the radio plasma. For a Galactic rotation velocity $v_r \sim 220 \text{ km s}^{-1}$ (which sets the vertical gravity g_z), a Galacto-centric distance of $r \sim 10 \text{ kpc } r_{10}$ (where r_{10} is the Galacto-centric distance in units of 10 kpc), and a vertical trail position $z \sim 200 \text{ pc } z_{0.2}$ above the Galactic mid-plane (where $z_{0.2}$ is the trail height in units of 200 pc), and assuming a drag coefficient C_W of about 1 for a cylindrical trail, the buoyancy speed is

$$\begin{aligned} v_B &\approx \sqrt{\frac{g_z \pi R}{C_W}} \approx \frac{v_{\text{rot}}}{r} \sqrt{\pi R z} \quad (21) \\ &\approx 3 \times 10^5 \text{ cm s}^{-1} \cdot \frac{z_{0.2}^{1/2}}{r_{10}} \left(\frac{W_{37}}{p_{-11.5} v_{17}} \right)^{1/4} \mathcal{R}^{-1/16} \end{aligned}$$

For a disk scale height of $H \approx 500 \text{ pc } H_{0.5}$, the buoyancy time is

$$\begin{aligned} \tau_b &\sim H/v_B \quad (22) \\ &\approx 1.6 \times 10^8 \text{ yrs} \cdot \frac{r_{10} H_{0.5}}{z_{0.2}^{1/2}} \left(\frac{p_{-11.5} v_{17}}{W_{37.3}} \right)^{1/4} \mathcal{R}^{-1/16} \end{aligned}$$

which is, by default, longer than a sound crossing time (since buoyancy is always sub-sonic). This is comparable to the lifetime of an HMXB, but could be short compared to the lifetime of an LMXB.

Unhindered, this process will eventually remove all of the radio plasma from the disk into the halo. However, a number of processes will work against this transport out of the plane, trying to mix the relativistic plasma into the ISM. In order to estimate their importance, one needs to compare the time scales over which they act to the buoyancy time. If they are occurring on more rapid time scales, they might mix a significant amount of radio plasma macroscopically with the ISM before it has time to escape into the halo, especially because all of these processes will only increase the trails surface area and thus its buoyancy time. At the same time, an increase in surface area will also increase the microscopic mixing fraction f_{mix} .

3.3.2. Shredding

Due to the differential rotation of the Galaxy, any object of finite size will experience Galactic shear. Since the radio trails are embedded in the ISM, they will be affected.

Taking the Galactic rotation velocity $v_r \sim 220 \text{ km s}^{-1}$ to be constant with radius, the angular velocity shear across the trail is $d\omega/dr = -v_r/r^2$. The Shredding time for an object much smaller than its Galacto-centric distance r that is subject to this shear is

$$\tau_{\text{shear}} \sim r/v_r \sim 5 \times 10^7 \text{ yrs} \cdot r_{10} \quad (23)$$

independent of the actual size of the object.

After several shredding times the object will have been significantly stretched and distorted and will eventually be mixed with the ISM. Note that the shredding time is approximately equal to the buoyancy time, so for an XRB in the Galactic

plane, it is plausible that shredding will distort, and possibly even destroy the radio trail before it can escape into the halo.

3.3.3. RT and KH instabilities

In addition to shear-shredding, the trails will also be subject to dynamical instabilities. The same buoyancy process that drives the trails out of the Galactic plane will also trigger the formation of Rayleigh-Taylor instability, acting to destroy the trail and macroscopically mix the radio plasma with the ISM. The growth time for a mode with wave number k is $\tau \sim \sqrt{gk}$ (for large density contrast between trail and ISM). Since the trails are filled with magnetized plasma, magnetic tension will suppress the growth of small wavelength modes. However, global modes will likely not be suppressed by tangled fields (at least in the linear regime), and so the growth time for a body mode with wave number $k = 2\pi/R_{\text{eq}}$ will be

$$\tau_{\text{RT}} \sim \sqrt{\frac{2\pi g}{R}} \sim \frac{r}{v_r} \sqrt{\frac{R}{2\pi z}} = \tau_b \frac{R}{H} \sqrt{\frac{1}{4C_W}} < \tau_b \quad (24)$$

with $C_W \sim 1$ being the drag coefficient. Thus, RT instability will set in well before buoyancy had time to remove the plasma out of the disk and into the Halo. If RT instability does grow at the hydrodynamic rate, it will fragment the radio trails into smaller pockets, which will be subject to further RT instability.

Eq. (24) shows that RT instability is more efficient the smaller the size of the plasma pocket, thus, if RT instability is not suppressed on scales comparable to R_{eq} by the presence of large scale magnetic fields, it will destroy the radio trail into a spectrum of bubbles small enough for magnetic tension to stabilize them before buoyancy transports the plasma out of the disk. Since the buoyancy time of smaller bubbles is longer, the RT fragmentation will delay buoyant transport and give other processes more time to act and, by increasing the surface area of the plasma, increasing the efficiency of diffusive processes.

In addition to RT instability, Galactic differential rotation and buoyancy drift will induce KH instability along the edge of the trail. The typical velocities encountered are of order $v_{\text{buoy}} \sim v_r \sqrt{Rz}/r$ and $v_{\text{shear}} \sim 2v_r R/r$. v_{shear} will dominate at early times, v_{buoy} will become larger after a few buoyancy times. Taking the relativistic inertia of the radio plasma into account, the KH growth time of a body mode with $\lambda \sim R$ is roughly

$$\tau_{\text{KH}} \sim \sqrt{\frac{R^2}{v_{\text{buoy}}^2 + v_{\text{shear}}^2} \frac{\rho_{\text{ISM}} c^2}{4p_{\text{ISM}}}} \quad (25)$$

$$\sim R\tau_b \tau_{\text{shear}} \sqrt{\frac{5}{12(H^2 \tau_{\text{shear}}^2 + z^2 \tau_b^2)} \frac{c}{c_{\text{sound}}}} \quad (26)$$

Clearly, the ratio c/c_{sound} is much larger than either z/R or H/R for typical trail radii (see eq. 12), and KH instability should not contribute much to the global destruction of radio bubbles and trails. However, it could well induce a spectrum of short wavelength modes that creates a shear layer around the trail, where efficient mixing between the two phases occurs.

3.4. The impact on the ISM: Magnetization and cosmic ray seeding

Given the total volume of plasma released by XRBs and some value of f_{mix} , we can estimate the strength of the magnetic field that is released and seeded into the ISM.

We will use the expression for the field strength inside the trail from eq. (17). Further assuming magnetic flux conservation, the strength of the magnetic field after the residual fraction f_{mix} of the radio plasma is mixed with the ISM is

$$\begin{aligned} B_{\text{mixed}} &\approx f_{\text{mix}} B_{\text{eq}} & (27) \\ &\sim 11 f_{\text{mix}} \mu\text{G} \cdot \sqrt{\frac{2\xi_B}{p_{-11.5} (1 + \xi_B)}} b \\ b &\equiv \frac{5.5 W_{\text{L},38.5} f_{\text{disk},75} t_{10} h_{\text{L}} + 4 W_{\text{H},38.3} M_{11} h_{\text{H}} / \dot{M}_3}{9.5} \end{aligned}$$

where b is unity for the set of fiducial parameters. Since t_{10} and M_{11} enter linearly into this expression, the magnetic field provided by XRB jets will have been linearly increasing as a function of time for most of the Galactic history, but will have been increasing more rapidly during intense star formation episodes, when M increased dramatically, since then the HMXB population would have been much more numerous.

This should be compared to an estimated mean Galactic field of order $B_{\text{G}} \sim 10 \mu\text{G}$ (e.g. Wentzel 1963), which is believed to have been created by dynamo action on a small seed magnetic field. Comparing both values implies that $f_{\text{mix}} \sqrt{2\xi_B/[p_{-11.5}(1 + \xi_B)]} b < 1$, which is easily satisfied since we estimated $f_{\text{mix}} \lesssim 0.04$ above.

The seed field required to produce the observed Galactic field is rather small ($B_{\text{seem}} \sim 10^{-17} \text{G}$ Anderson 1992). Even under the most conservative assumptions possible — mixing of only one skin depth of the thickness of one proton gyro radius ($f_{\text{mix}} \sim 10^{-9}$) — such a field strength could have been provided by XRB jets within about 10^5 yrs after the first XRBs turned on (though it would need a few Galactic revolutions of duration $\tau_{\text{rev}} \sim 2.5 \times 10^8$ yrs to get spread over a significant fraction of the disk). More reasonable choices of f_{mix} imply that the strength of the seed field provided by XRB jets is likely orders of magnitude larger. In fact, given the numbers derived above, is likely that the strength of the field seeded by XRB jets is only about two orders of magnitude below the observed mean Galactic value.

Of particular importance in this case is the fact that LMXBs travel far from their birthplaces, leaving behind trails of magnetized plasma, which should permeate the Galactic plane more or less uniformly (modulated by the average space density as a function of Galacto-centric distance).

Since XRB production is an unavoidable part of star formation (Grimm et al. 2002) and since jet activity is an integral part of XRB activity (e.g. Fender 2001), it is clear that jets must play a role in providing magnetic fields in forming galaxies and the cumulative effect of XRBs on the ISM implies that they are likely responsible for a non-negligible fraction of the field in mature galaxies as well.

Along with the magnetization, it is clear that relativistic particles from within the lobe will mix into the interstellar medium as cosmic rays. This process was discussed in more detail in Heinz et al. (2002). A critical question raised in that paper was the adiabatic cooling of these particles. The pressure inside the working surface has already been estimated in eqs. (7) and the pressure inside the trail/lobe to which the cosmic ray plasma has to expand is simply the ISM pressure.

Taking the bulk of the particles leaving the working sur-

face to have energies comparable to the randomized specific kinetic energy of the jet, i.e., $\gamma \sim \Gamma$, the final energy of any cosmic ray protons in the trails is

$$E_{\text{CR}} \approx \gamma m_p c^2 \left(\frac{p_{\text{ISM}}}{p_{\text{dyn}}} \right)^{\frac{1}{4}} \approx 3.3 \text{ GeV} \cdot \Gamma_5 \mathcal{R}^{\frac{1}{4}} \quad (28)$$

indicating that adiabatic losses are likely small enough to leave the results regarding the total energetic of cosmic ray injection by microquasars discussed in Heinz et al. (2002) unchanged: the total energetics of microquasars is likely to contribute of order a few percent to the Galactic cosmic ray population. Thus, microquasars located in the vicinity of molecular clouds should be observable through gamma-ray emission due to hadronic interaction with the cloud protons detectable by GLAST. A corollary of this process is GeV neutrino emission that should also arise. The high energy tail from this emission might be detectable with high energy neutrino detectors like Ice Cube.

4. OBSERVABILITY

Given the estimated pressure and size of the plasma trails and working surfaces (i.e., hot spots), we can estimate their synchrotron luminosity and surface brightness. We once again use the expression from eq. (17) to parameterize the field strength. Since it is unclear what the composition of the plasma is (e^+/e^- vs. p^+/e^-), we parameterize the proton pressure as $p_p = \xi_p p_{\text{tot}} / [(1 + \xi_B)(1 + \xi_p)]$, where ξ_p is the ratio of proton to lepton pressure.

4.1. Radio trails

While the field strength we estimate for the trails is not much larger than the mean Galactic field, it is safe to assume that the partial pressure from relativistic electrons inside the trails is larger than outside, implying that the trails will produce synchrotron emission that is significantly enhanced over the mean Galactic emission.

For a powerlaw distribution of electrons with index 2 such that $dN/d\gamma \propto \gamma^{-2}$, the synchrotron emissivity of the plasma is (Rybicki & Lightman 1979)

$$\epsilon_\nu \approx \frac{5 \times 10^{-38} \text{ ergs}}{\text{cm}^3 \text{ s Hz}} \cdot \left(\frac{2p_{-11.5}}{1 + \xi_B} \right)^{\frac{7}{4}} \frac{2\xi_B^{3/4}}{1 + \xi_p} \sqrt{\frac{\nu}{5 \text{ GHz}}} \quad (29)$$

The magnetic field strength inside the trail is approximately $B_{\text{eq}} \approx 1.4 \times 10^{-5} \text{ mG } p_{-11.5} 2\xi_B / (1 + \xi_B)$, which gives a cooling time of

$$\tau_{\text{cool}} \sim 10^7 \text{ yrs} \cdot \left[\frac{1 + \xi_B}{2\xi_B p_{-11.5}} \right]^{3/2} \nu_5^{-1/2} \quad (30)$$

for an electron emitting at frequency $\nu \equiv 5 \text{ GHz } \nu_5$. The length of radio trail a particle can travel before cooling losses affect it is

$$l_{\text{cool}} \sim \tau_{\text{cool}} v_{\text{XRB}} \approx 5 \times 10^{20} \text{ cm} \cdot \left[\frac{1 + \xi_B}{2\xi_B p_{-11.5}} \right]^{3/2} \frac{v_{17} \mathcal{V}}{\nu_5^{1/2}} \quad (31)$$

which is comparable to R_{eq} from eq. (12). Thus, the trails left behind by XRBs should typically only emit at frequencies well below 5GHz. Above such frequencies, the radio emission from XRBs should be concentrated around the XRB itself. Given their large angular sizes and low frequency emission, these trails will be ideal targets for the new wave of

high fidelity, low frequency radio arrays, such as LOFAR, the LWA, the MWA, and, ultimately, the SKA-low.

The central surface brightness of a given trail within a cooling distance l_{cool} from the XRB will be

$$\Sigma \approx 2R_{\text{eq}} \epsilon \quad (32)$$

$$\approx \frac{4\mu\text{Jy}}{\text{arcsec}^2} \left[\frac{2}{1 + \xi_B} \right]^{\frac{7}{4}} \frac{2p_{-11.5}^{\frac{5}{4}} \xi_B^{\frac{3}{4}}}{1 + \xi_p} \sqrt{\frac{W_{37.3}}{\nu_5 v_{17} \mathcal{V}}} R_M^{-\frac{1}{8}}$$

and the integrated trail luminosity at a fixed frequency is

$$L_\nu \approx \pi R_{\text{eq}}^2 l_{\text{cool}} \epsilon_\nu = 3 \times 10^{24} \text{ ergs Hz}^{-1} \text{ s}^{-1} \cdot \nu_5^{-1} \quad (33)$$

While every microquasar should have some kind of radio lobe/trail in its vicinity, some sources will be better suited to study this effect than others. Cygnus X-1, for example, is already known to possess a dark radio lobe. As an HMXB with a relatively young age, it is unlikely to show much of a radio trail, as argued above, and indeed, the radio lobe seems to be close to the source, though it does show a one-sided asymmetry: the radio ring surrounding it that led to the claim of the radio lobe is one-sided. This asymmetry could be due to the fact the source is located at the border of a high density cloud.

Arguably one of the best sources to look for a radio trail is XTE J1118+480, which is known to have both a steady low/hard state jet as well as a large space velocity (Mirabel et al. 2001). We suggest that this should be one of the first targets to study with low frequency, large scale radio mapping for evidence of a plasma trail.

The large scale, asymmetric radio emission recently detected surrounding Cygnus X-3 (Sánchez-Sutil et al. 2008) is also suggestive and we interpret it as dynamical interaction with the ISM. The overall morphology suggests that the source is moving in a roughly northern direction relative to the ISM. This should be followed up with VLBI proper motion measurements of the XRB itself to test this hypothesis.

4.2. Hot spots

Given the estimate of the jet length l_{jet} from eq. (8) and the pressure inside the working surface, we can estimate the order of magnitude of the synchrotron emission from each hot spot as $L_{\nu, \text{HS}} \approx \epsilon_\nu \frac{4\pi(\alpha l)^3}{3}$. Once the plasma has moved out of the working surface of a jet, it expands (i.e., cools) adiabatically and reaches pressure equilibrium with the lobe. The pressure inside the hot spot is given by

$$p_{\text{HS}} \approx \frac{W_{\text{jet}}}{2\pi(\alpha l_{\text{jet}})^2 c} \quad (34)$$

giving an approximate the hot spot luminosity of

$$L_{\text{HS, mu}} \approx \epsilon_\nu \frac{4\pi(\alpha l)^3}{3} \quad (35)$$

$$\approx 4 \times 10^{19} \text{ ergs s}^{-1} \text{ Hz}^{-1} \frac{W_{37}^{3/2} p_{-11.5}^{1/4} \theta_{20}^{1/2}}{\alpha_1^{1/2}} \cdot \left(\frac{28\Gamma\beta_{\text{jet}}\mathcal{R}_M}{25\Gamma + 15} \right)^{1/4}$$

For typical microquasar parameters, the synchrotron cooling time τ_X for X-ray emitting electrons is longer than the adiabatic cooling time and the same expression should hold for radio as well as X-ray synchrotron emission. This flux

is accessible with *Chandra* and in fact has been observed in a number of cases, most notably XTE J1550 (Corbel et al. 2002). In the case of XTE J1550, the hot spot has been observed to move away from the XRB at mildly relativistic speeds, which fits in well with the picture developed here: If the jet power rises sharply, as indicated by the radio flares that precede the detection of the hot spots, the working surface will (a) brighten and (b) move outward, decelerating as it moves into undisturbed ISM. The distances where the hot spots are observed are consistent with where we would expect them from equation (8).

4.3. Bow shocks and shells

As has been discussed in the literature (Gallo et al. 2005; Russell et al. 2007), and as is observed around radio galaxies in clusters (e.g. Birzan et al. 2004) the source will sweep up a quasi-spherical shell during its initial inflation. This shell will emit thermal bremsstrahlung, potentially up to X-ray energies, as well as line emission from the shocked plasma.

For the early, quasi-spherical evolution and for stationary source, we refer the reader to the discussion in the context of expanding shells in galaxy clusters (e.g. Heinz et al. 1998) and binaries (Heinz et al. 2006a) and concentrate on the emission from the ISM swept up ahead of radio trails in the case of XRBs with appreciable space velocity.

Given that LMXB space velocities top out at a few hundred km/s, we should expect temperatures up to about a keV, which should be detectable by X-ray telescopes (which is also the case in pulsar-wind nebulae). The radiative cooling time strongly depends on the ISM density, but assuming that the shock is fully radiative gives an upper limit on the total luminosity from the swept up ISM of

$$L_{\text{shock}} < \pi R_{\text{eq}}^2 \frac{\rho_{\text{ISM}} v_{\text{XRB}}^3}{2} \quad (36)$$

$$\approx 5 \times 10^{35} \text{ ergs s}^{-1} \cdot v_{17}^2 n_1 \frac{W_{37}}{p_{-11.5} \mathcal{V} \mathcal{R}^{1/4}}$$

spread over a region close to a degree in size (thus hard to detect with the typical field of view of current X-ray instruments).

Longer wavelengths seem more suitable for finding these thermal sources (specifically, narrow band imaging of promi-

nent shock-excited lines on degree scales, as well as broadband imaging to look for free-free emission Russell 2008). Given that the estimated expansion velocity of the shell around Cyg X-1 is of order a few dozen km/s, we would expect surface brightness and total power to be comparable with those detected in the Cyg X-1 nebula. This suggests that asymmetric bow shock emission might be a suitable way to identify sources for low frequency follow up.

5. CONCLUSIONS

We proposed that jets from X-ray binaries (microquasars) leave behind trails of non-thermal, synchrotron emitting plasma as they move through the interstellar medium. LMXBs are more likely to leave such trails due to their longer life expectancy and, more importantly, due to the higher expected space velocities, while HMXBs likely produce more stationary radio lobes.

The total plasma volume deposited by XRBs over the history of the Galaxy is comparable to the total disk volume and constitutes a non-negligible fraction of the halo volume. We argue that a fraction f_{mix} of order a few percent of this plasma is mixed into the thermal ISM.

The magnetic field thus released can easily provide the seed field for Galactic dynamos to produce the fields observed in spiral galaxies even under the most conservative assumptions. Since HMXBs turn on rapidly after an episode of star formation, this mechanism should be important for galactic magnetic field production and maintenance within a time frame of about 10^7 yrs from the first supernovae.

We showed that radio emission from the plasma inside the trail should be visible primarily at low frequencies, since the radiative cooling time of the plasma at GHz frequencies limits emission to a roughly spherical region around the binary. LOFAR, MWA, LWA and other future low frequency, wide field instruments are ideally suited for searches of this emission. LMXBs with high detected proper motions like XTE J1118+480 will be the best candidates for such a search.

We would like to thank A. Merloni and C. Kaiser for helpful discussions. S.H. acknowledges support from NSF astrophysics grant 0707682.

REFERENCES

- Anderson, S. W. 1992, Ph.D. Thesis
- Birzan, L., Rafferty, D. A., McNamara, B. R., Wise, M. W., & Nulsen, P. E. J. 2004, *ApJ*, 607, 800
- Begelman, M. C. & Cioffi, D. F. 1989, *ApJ*, 345, L21
- Blandford, R. D. & McKee, C. F. 1976, *Physics of Fluids*, 19, 1130
- Bucciantini, N., Amato, E., & del Zanna, L. 2005, *A&A*, 434, 189
- Castor, J., McCray, R., & Weaver, R. 1975, *ApJ*, 200, L107
- Corbel, S., Fender, R. F., Tzioumis, A. K., Tomsick, J. A., Orosz, J. A., Miller, J. M., Wijnands, R., & Kaaret, P. 2002, *Science*, 298, 196
- Cordes, J. M. 1996, in *ASP Conf. Ser. 105: IAU Colloq. 160: Pulsars: Problems and Progress*, 393
- Cox, D. P. 2005, *ARA&A*, 43, 337
- Dalgarno, A. & McCray, R. A. 1972, *ARA&A*, 10, 375
- Draine, B. T., Roberge, W. G., & Dalgarno, A. 1983, *ApJ*, 264, 485
- Elmegreen, B. G. 1979, *ApJ*, 232, 729
- Fender, R., Maccarone, T., & Kesteren, Z. 2005, *MNRAS*, in press, press
- Fender, R. P. 2001, *MNRAS*, 322, 31
- Fender, R. P., Belloni, T. M., & Gallo, E. 2004, *MNRAS*, 355, 1105
- Fender, R. P. & Hendry, M. A. 2000, *MNRAS*, 317, 1
- Fender, R. P. & Kuulkers, E. 2001, *MNRAS*, 324, 923
- Frail, D. A., Giacani, E. B., Goss, W. M., & Dubner, G. 1996, *ApJ*, 464, L165+
- Frank, J., King, A., & Raine, D. 2002, *Accretion power in astrophysics*. 3rd ed. (Cambridge, UK: Cambridge University Press. ISBN 0-521-62957-8, 2002, XIV + 384 pp.)
- Gallo, E., Fender, R., Kaiser, C., Russell, D., Morganti, R., Oosterloo, T., & Heinz, S. 2005, *Nature*, 436, 819
- Gallo, E., Fender, R. P., & Pooley, G. G. 2003, *MNRAS*, 344, 60
- Grimm, H.-J., Gilfanov, M., & Sunyaev, R. 2002, *A&A*, 391, 923
- Heiles, C. & Troland, T. H. 2003, *ApJ*, 586, 1067
- Heinz, S., Aloy, M. A., Fender, R. P., & Russell, D. M. 2006a, in *VI Microquasar Workshop: Microquasars and Beyond*
- Heinz, S. & Begelman, M. C. 2000, *ApJ*, 535, 104
- Heinz, S., Brügggen, M., Young, A., & Levesque, E. 2006b, *MNRAS*, in press
- Heinz, S., Choi, Y., Reynolds, C. S., & Begelman, M. C. 2002, *ApJ*, 569, L79
- Heinz, S. & Grimm, H. 2005, *ApJ*, 644, 384
- Heinz, S., Reynolds, C. S., & Begelman, M. C. 1998, *ApJ*, 501, 126
- Heinz, S. & Sunyaev, R. A. 2003, *MNRAS*, 343, L59
- Kaiser, C. R. & Alexander, P. 1997, *MNRAS*, 286, 215
- Kaiser, C. R., Gunn, K. F., Brocksopp, C., & Sokolowski, J. L. 2004, *ApJ*, 612, 332
- McKee, C. F. & Ostriker, J. P. 1977, *ApJ*, 218, 148

- McNamara, B. R. & Nulsen, P. E. J. 2007, *ARA&A*, 45, 117
- Miley, G. 1980, *ARA&A*, 18, 165
- Mirabel, I. F., Dhawan, V., Mignani, R. P., Rodrigues, I., & Guglielmetti, F. 2001, *Nature*, 413, 139
- Narayan, R. & Medvedev, M. V. 2001, *ApJ*, 562, L129
- Odea, C. P. & Owen, F. N. 1986, *ApJ*, 301, 841
- Reynolds, C. S., Heinz, S., & Begelman, M. C. 2002, *MNRAS*, 332, 271
- Russell, D. 2008, *ArXiv e-prints*, 802
- Russell, D. M., Fender, R. P., Gallo, E., & Kaiser, C. R. 2007, *MNRAS*, 376, 1341
- Rybicki, G. B. & Lightman, A. P. 1979 (New York: Wiley)
- Sánchez-Sutil, J. R., Martí, J., Combi, J. A., Luque-Escamilla, P., Muñoz-Arjonilla, A. J., Paredes, J. M., & Pooley, G. 2008, *A&A*, 479, 523
- Scheuer, P. A. G. 1982, in *IAU Symp. 97: Extragalactic Radio Sources*, ed. D. S. Heeschen & C. M. Wade, 163–165
- Shu, F. 1992, "The Physics of Astrophysics" (University Science Books, Sausalito, California)
- Wentzel, D. G. 1963, *ARA&A*, 1, 195
- Young, A. J., Wilson, A. S., Tingay, S. J., & Heinz, S. 2005, *ApJ*, 622, 830